Lawrence Berkeley National Laboratory

Title

On scale and magnitude of pressure build-up induced by large-scale geologic storage of CO2

Permalink

https://escholarship.org/uc/item/8jd2d5x7

Author

Zhou, Q.

Publication Date

2011-06-01

DOI

DOI: 10.1002/ghg3.001

On Scale and Magnitude of Pressure Buildup Induced by Large-Scale Geologic Storage of CO_2

Quanlin Zhou * and Jens T. Birkholzer

Earth Sciences Division, Lawrence Berkeley National Laboratory, University of California, Berkeley, CA 94720

*Corresponding Author, Tel: 1-510-486-5748, Fax: 1-510-486-5686; Email: qzhou@lbl.gov, Mail Address: One Cyclotron Road, MS 90-1116

Abstract

The scale and magnitude of pressure perturbation and brine migration induced by geologic carbon sequestration is discussed assuming a full-scale deployment scenario in which enough CO_2 is captured and stored to make relevant contributions to global climate change mitigation. In this scenario, the volumetric rates and cumulative volumes of CO_2 injection would be comparable to or higher than those related to existing deep-subsurface injection and extraction activities, such as oil production. Large-scale pressure buildup in response to the injection may limit the dynamic storage capacity of suitable formations, because over-pressurization may fracture the caprock, may drive CO_2/brine leakage through localized pathways, and may cause induced seismicity. On the other hand, laterally extensive sedimentary basins may be less affected by such limitations because (1) local pressure effects are moderated by pressure propagation and brine displacement into regions far away from the CO_2 storage domain, and (2) diffuse and/or localized brine migration into overlying and underlying formations allows for pressure bleed-off in the vertical direction. A quick analytical estimate of the extent of pressure buildup induced by industrial-scale CO_2 projects is presented. Also discussed are pressure perturbation and attenuation effects simulated for two representative sedimentary basins in the U.S.: the laterally extensive Illinois Basin and the partially compartmentalized southern San Joaquin Basin, California. These studies show that the limiting effect of pressure buildup on dynamic storage capacity is not as significant as suggested by Ehlig-Economides and Economides [1], who considered closed systems without any attenuation effects.

Keywords: climate change, geologic sequestration, storage capacity, pressure buildup, numerical modeling, pressure attenuation

1. Introduction

Pressure buildup caused by the injection of CO_2 into deep brine-filled aquifers is of great importance to the safety of geologic carbon sequestration (GCS) projects. Excessive pressurization may (1) fracture the caprock because of mechanical damage, (2) drive brine upward through localized pathways into shallower groundwater resources, and (3) cause induced seismicity. Efforts to reduce these environmental risks by limiting injection pressure will impact the effective storage capacity of sedimentary basin formations. Large-scale aquifer pressurization has become an issue in operating industrial-scale storage projects, because the combined annual injection rate of these storage projects is about two million metric tons (Mt) CO_2, excluding enhanced oil recovery operations [2]. When carbon capture and storage (CCS) and GCS are approaching full deployment in the future, large-scale pressure buildup will have to be addressed.

The pressure response to CO_2 storage will depend on the boundary conditions of the storage reservoir, here defined by three storage-system end members: (1) a closed system in which the storage formation is surrounded laterally by impervious boundaries and vertically by impervious sealing units, (2) a semi-closed system in which the storage formation is bounded laterally by impervious boundaries, but is overlain and/or underlain by semi-pervious sealing units, and (3) an open system whose lateral boundaries are so far away that they remain unaffected by pressure perturbations [3]. Recent modeling studies on open systems have indicated that the storage capacity for CO_2 may be limited by pressure effects in response to the injection and storage of additional fluid volumes, because the pressure buildup in a storage formation cannot exceed a maximum tolerable pressure gradient that would assure geomechanical integrity of the caprock [4-6]. Brine migration through localized pathways (e.g., leaky faults and wells) driven by elevated pressure may degrade shallower groundwater resources, further limiting effective storage capacity. On the other hand, pressure bleed-off caused by diffuse brine migration into and through semi-pervious sealing units and/or by lateral brine displacement in the storage formation may enhance the effective storage capacity of an open or a semi-closed system. Reservoir pressurization is effectively reduced by such brine migration, while environmental impact on overlying groundwater resources is typically not of concern due to the very small flow velocity and displacement length [7].

In closed (compartmentalized) systems, the limiting effect of pressure buildup on storage capacity is more apparent than in semi-closed and open systems because of the lack of pressure bleed-off [1, 3], although no environmental risk exists for brine leakage as long as the pressure buildup is less than the maximum tolerable pressure gradient. When these pressure constraints (as well as two-phase flow effects known to affect storage efficiency) are considered, the "dynamic" storage capacity is expected to be lower than the "static" storage capacity. The former is defined as the storage capacity that can be achieved during the active lifetime of the project by injecting CO_2 at rates and pressures that meet safety and regulatory requirements [8], while the latter represents the effective deep

2

subsurface pore volume available for CO_2 storage, without taking into account economic, regulatory, and/or environmental constraints. For example, the static storage capacity in deep saline aquifers in the U.S. is estimated to range between 3,297 and 13,909 billion metric tons (Gt) CO_2 for a 15 and 85% confidence range related to uncertainties in various parameters [9].

In order for CCS/GCS to play an important role in climate change mitigation, very large volumes of captured CO_2 will need to be injected and stored in deep saline aquifers. It is thus important to understand the scale and magnitude of the pressure perturbations generated from CCS/GCS operations. In this paper, we review some existing analogue injection and production operations and their pressure impacts, present estimates of the spatial scale and magnitude of pressure perturbations based on analytical expressions, and finally show some state-of-the-art simulations of CO_2 injection into prospective storage formations in the U.S. These results will serve to demonstrate that, while pressure buildup can extend over large areas, it tends to be moderated by open-system behavior in natural systems wherein brine migration serves to accommodate the injected CO_2 volume.

2. Scale of Pore Volume Needed for Geologic Carbon Storage

Before discussing pressure effects, we shall briefly review the magnitude of subsurface pore volume needed for CCS/GCS to significantly reduce CO_2 emissions, relative to other fluid injection-extraction activities. Figure 1a shows the annual volume of world oil production and the pore volume needed to store annual energy-related CO_2 emissions, assuming that the CO_2 is stored in the subsurface at a density of 700 kg/m^3. In 2006, the world oil production was 4.3 km^3 (73.46 million barrel/day), accompanied by produced water, with an average water-to-oil ratio of 3 to 1 [10]. Considering that the produced water is generally re-injected into the subsurface for water flooding, enhanced oil recovery, and disposal, the net cumulative effect on subsurface pore volume is mainly from oil production. The equivalent volume for worldwide CO_2 emissions was 41.7 km^3 (29.2 Gt CO_2/year) in 2006. This means that the subsurface pore volume needed for CO_2 storage with zero energy-related emissions exceeds the total volume of world oil production by a factor of ten. This ratio increases with time, as shown in Figure 1a.
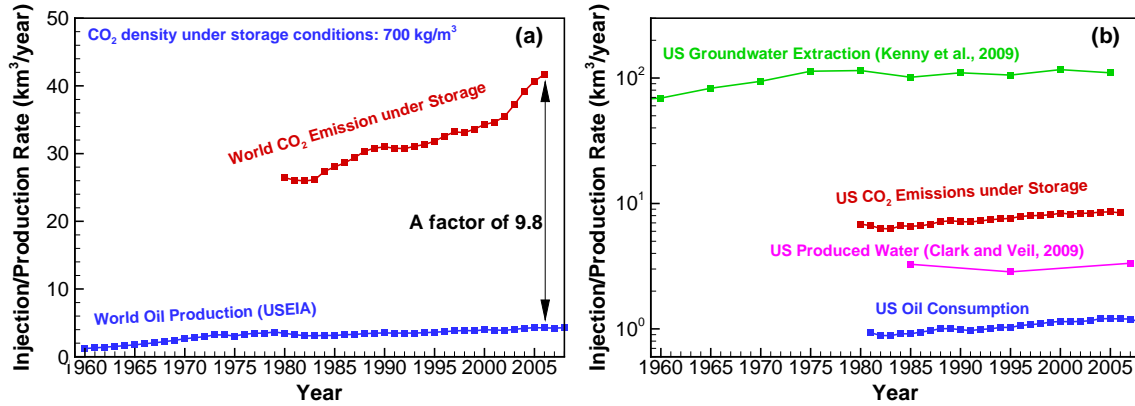
Figure 1. Comparison of the annual pore volumes needed to sequester 100% CO_2 emissions at an assumed density of 700 kg/m³ for (a) the world and (b) the United States, to the annual volumes of world oil production and U.S. oil consumption, as well as produced water with oil/gas production [11-12] and fresh groundwater extraction in the U. S. [13]. All other data are obtained from USEIA [14]. Note that the log scale is used for the y-axis in (b).

In the U.S., the ratio of the equivalent storage volume of 8.4 km³ for CO_2 emissions (5.9 Gt CO_2) to crude oil consumption of 1.2 km³ (7.55 billion barrels) was 7.0 in 2006. Only 3.8 Gt of CO_2 emissions could be captured from stationary sources [9], which reduced the equivalent storage volume to 5.4 km³. The combined U.S. production rate of crude oil (0.3 km³) and produced water (3.3 km³) in 2007 [12] was within around 67% of the annual storage volume required for point-source CO_2 storage. However, because 95% of the produced water is re-injected, the cumulative pore volumes affected and fluid pressure perturbations caused by the oil industry are significantly smaller than those expected from full-scale deployment of GCS in deep formations.

The largest injection-extraction activity in the U.S. is fresh groundwater withdrawal for water supply. The total extraction volume was 110.0 km³ (79.6 billion gallons/day) in 2005 [13], approximately 20 times larger than the equivalent storage volume for all of the CO_2 from U.S. stationary sources In terms of pressure impacts and aside from the fact that one activity involves withdrawal and the other injection, there are two major differences between groundwater supply and GCS: (1) groundwater supply is mainly from shallow freshwater aquifers, while GCS will mainly occur in deep saline aquifers that have lower pore compressibility (i.e., resulting in more significant pressure change), and (2) shallow freshwater aquifers replenish from natural recharge due to precipitation, which offsets, at least partially, water withdrawal. Therefore, GCS may result in more significant pressure perturbations than freshwater supply from shallow resources, even though the former moves fluid volumes 20 times less than the latter.

Through these comparisons, it appears that the pore volume needed for CO_2 storage in a full-scale deployment scenario (i.e., with capture from all point sources) may be up to an order of magnitude larger than the net fluid volume extracted for world oil production. In

the following, the scale and magnitude of pressure perturbations caused by GCS are analyzed by analytical and numerical approaches.

3. Scale and Magnitude of Pressure Buildup

For a given injection scenario, the scale (radial distance from injection site) of pressure buildup depends on the geometric and hydrogeologic properties of the storage formation and its neighboring formations. The relevant physical processes include (1) lateral propagation of pressure buildup within the storage formation away from injection sites to the margins of a sedimentary basin, (2) attenuation of pressure buildup caused by basin-scale migration of resident brine into and through the caprock and basement rock, (3) superposition of pressure buildup from neighboring injection sites [6], and (4) boundary effects at basin margins. Such boundary effects are apparent in a closed or partially closed storage system [3,15]. Brine may leave the storage formation due to diffuse migration into and through seals of low but nonzero permeability [7], and/or focused leakage through leaky wells and faults [16]. The leaky wells may either pre-date GCS activities or may be developed specifically for pressure management and mitigation to reduce pressure effects and enhance storage capacity. The magnitude of pressure buildup in CO_2 plumes also depends on the characteristics of the two-phase CO_2-brine flow and is ultimately constrained by the maximum tolerable pressure gradient.

The radial scale of pressure buildup induced by continuous, constant-rate injection in a single well can be approximated using simple analytical solutions. We may define a dimensionless pressure buildup of $p_D(U_F) = 0.05$ as the cut-off value for the arrival of a pressure wave, where U_F is the cut-off value of the dimensionless similarity variable U ($= R^2/4D_h t$), D_h is the horizontal hydraulic diffusivity, R is the radial distance from the injection well, and t is the time. The corresponding radial scale (R_F) can be estimated using $R_F(t) = \sqrt{4U_F D_h t}$. For the case of impervious sealing units overlying and underlying the storage formation, $U_F = 2.0$ (from the well function), and $R_F(t) = \sqrt{8D_h t}$. For example, the radial scale is ~190 km at 50 years for $D_h = k_h/\phi\mu_b(\beta_b + \beta_p) = 2.8$ m^2/s, which is based on assuming a horizontal permeability $k_h = 10^{-13}$ m^2, porosity $\phi = 0.10$, brine viscosity $\mu_b = 0.5 \times 10^{-3}$ Pa·s, pore compressibility $\beta_p = 3.7 \times 10^{-10}$ Pa^{-1}, and brine compressibility $\beta_b = 3.4 \times 10^{-10}$ Pa^{-1}. For the case of storative and permeable sealing units, p_D and U_F are also a function of a dimensionless leakage factor and a dimensionless storage factor [17]. The radial scale is smaller than for the impervious sealing units, because of brine storage in and diffuse brine leakage through the seals. These estimates are based on the assumption of a vertical pressure equilibrium. The maximum time scale to reach a vertical quasi-equilibrium condition can be estimated as $t_{eq} = 2B^2/D_v$, where D_v is the vertical hydraulic diffusivity, and B is the thickness of the formation [18]. For example, using $D_v = 0.28$ m^2/s and $B = 300$ m yields an equilibration time of $t_{eq} = 7.4$ days. Thus, for most practical

purposes, the lateral pressure propagation can be solved as a one-dimensional radial flow, coupled with one-dimensional vertical flow through sealing units.

The time scale (t_{cp}) for a pressure perturbation to fully penetrate through a low-permeability seal can be estimated as $t_{cp} = 0.05B_s^2/D_{vs}$ given by Crank (p. 50) [18], where B_s and D_{vs} are the thickness and the vertical hydraulic diffusivity of the seal. The time scale (t_{ss}) for the pressure profile to reach steady-state conditions in the seal (a linear profile) can be estimated as $t_{ss} = 0.45B_s^2/D_{vs}$ given by Crank (p. 51) [18]. For a seal of $D_{vs} = 1.23 \times 10^{-7}$ m^2/s and B_s=100 m, with a relatively small vertical permeability of $k_v = 10^{-20}$ m^2, the two time scales are 130 and 1200 years, respectively. This means that brine leakage through a thick sealing unit with a very low permeability remains negligible over a long-time period after start of injection. The literature indicates that seal permeabilities can vary over a wide range from 10^{-16} to 10^{-23} m^2 [19]. For a seal with $D_{vs} = 1.23 \times 10^{-5}$ m^2/s, B_s=100 m, and $k_v = 10^{-18}$ m^2, the two time scales are 1.3 and 12.0 years, respectively. In this case, the storage in and diffuse leakage through the seal can play an important role in attenuating pressure buildup in the storage formation.

In these quick estimates of the scale of pressure buildup above, the idealized storage formation is assumed to be infinite laterally (i.e., an open system). In a closed or semi-closed system, the lateral scale of pressure buildup is constrained by the system boundaries after the pressure perturbation reaches these boundaries. As a result, the pressure buildup may be higher than in a laterally open system [1, 3, 17]. However, pressure bleed-off into overlying and underlying formations then becomes more important, in particular when the seal permeability exceeds 10^{-19} m^2, as shown by Zhou et al.[3] for a semi-closed system.

4. Pressure Buildup in Two Representative Sedimentary Basins

We present here two modeling studies illustrating the scale and magnitude of pressure buildup induced by industrial-scale CO_2 storage in the U.S. Two representative basins are considered, both of which are currently being investigated for large-scale demonstration and future GCS deployment. The pressure buildup (as well as CO_2 plume evolution) was simulated numerically based on detailed site characterization data. The first study considered a hypothetical future full-scale deployment scenario in the Mount Simon Sandstone in the Illinois Basin, which represents a laterally extensive open system [5-6]. The second case study involved CO_2 storage in the partially compartmentalized Vedder Sand in the southern San Joaquin Basin in California [15, 20]. The simulations were carried out using TOUGH2/ECO2N [21-22].

4.1. The Illinois Basin: An Open System

As shown in Figure 2a, the Mount Simon Sandstone is an extensive formation present in the entire Illinois Basin in Illinois and Indiana, with the exception of a small southern region where Precambrian hills exist. Salinity ranges from close to 268,000 mg litre^{-1} in

the deeper portions of the formation suitable for GCS to 300 mg litre^{-1} in the northern, shallow portion of the model domain. As a result, we use the term "brine" to refer to the resident fluid in this subsection. The formation further extends beyond the basin margins into neighboring states (e.g., Wisconsin and Kentucky). A few anticlines and faults are present in the model domain which comprises an area of 570 km by 550 km. However, there is no evidence that these structures affect regional groundwater flow in the deep Mount Simon Sandstone. In the core injection area which is most suitable for CO_2 storage, the thickness of the Mount Simon Sandstone varies from 300 to 700 m.
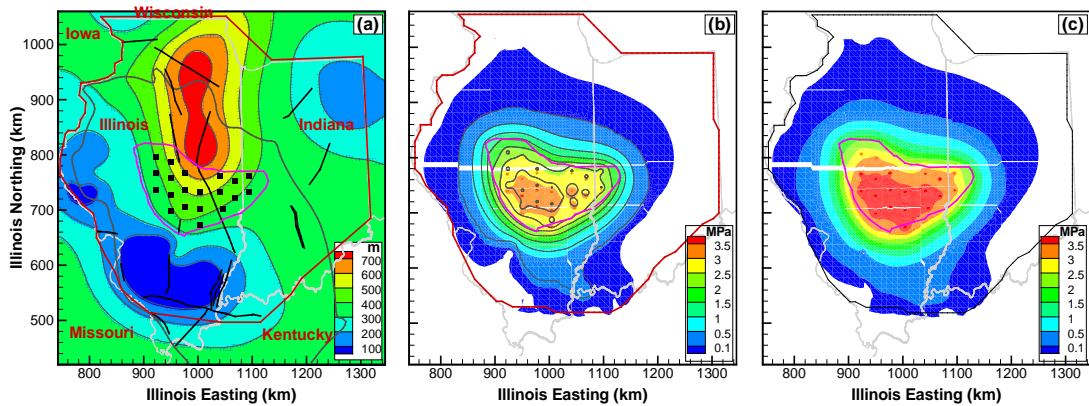

Figure 2. (a) Site map of the Illinois Basin, including the thickness (m) of the Mount Simon Sandstone (in flooded contour), saline basin boundary (gray polygons), major faults (thick black lines), state borders (thin gray lines), model boundary (thick red line), the core injection area (pink polygon), and 20 storage sites (black squares). Simulated pressure buildup (MPa) at 50 years of injection with diffuse leakage through caprock of a vertical permeability of (b) 10^{-18} and (c) 10^{-20} m^2. The cut-off pressure buildup is 0.01 MPa.

The hypothetical storage scenario for full-scale deployment of GCS in the Illinois Basin considered 20 individual storage projects, each injecting 5 Mt CO_2 per year for an injection period of 50 years. The total injection rate of 100 Mt CO_2/year corresponds to one third of the current annual emissions from large stationary CO_2 sources in the region [9]. The 20 projects (with a site spacing of ~30 km) are located in the core injection area in the basin center. Figure 2b shows the induced pressure buildup in the storage formation at the end of injection for a caprock permeability of 10^{-18} m^2 (the base case that best represents our understanding of basin-scale flow properties in the caprock). The maximum pressure buildup is 3.64 MPa in the core injection area, where strong interference between individual projects can be observed and the overall pressure response results from superposition of individual pressure impacts from each injection site. Very small pressure impacts appear along the western, northern, and southern boundaries, meaning that the formation acts like an open storage system during the injection period. For comparison, Figure 2c shows the simulated pressure buildup at 50 years for a caprock permeability of 10^{-20} m^2 (representative of core-scale data). The maximum pressure buildup is 4.36 MPa, 20% higher than in the base case. This result

suggests that pressure bleed-off can be a relevant attenuation factor even if seal permeability is quite low.

The total injected CO_2 mass in this scenario is 5 Gt after 50 years of injection. This mass is contained safely in the storage formation, mostly as supercritical CO_2 forming individual plumes ranging from 12 km to 14 km extent. At the end of injection, the average fractional pressure buildup (the ratio of pressure buildup to pre-injection pressure) at the injection centers is 0.18 (in the base case). This value is slightly higher than the 0.13 level that is commonly used for natural gas storage fields in Illinois and Indiana. However, it is only 28% of the regulated value of 0.65 at which geomechanical damage may start to occur, meaning the maximum dynamic storage capacity of the Mount Simon Sandstone is much higher than in the current storage scenario.

To extrapolate maximum dynamic storage capacity from the simulation results, we may either increase the total injection rate while keeping the injection time unchanged, or increase the injection time while keeping the injection rate unchanged. In the former, the injection rate could be increased by a factor of 3.6 before exceeding the regulated fractional pressure buildup. (This is based on the fact that pressure buildup is proportional to injection rate.) This increase would result in a dynamic storage capacity of 18.1 Gt CO_2, less than the estimated static storage capacity of the Mount Simon Sandstone, which ranges from 27 to 124 Gt CO_2 for a confidence range between 15 and 85% [9]. In the latter, the injection time could be increased up to 1200 years while keeping the fractional pressure buildup lower than the regulated value. (This calculation is based on a linear correlation between pressure buildup and $\log(t)$ at later time; see Figure 9a in Zhou et al.[6].) This leads to a dynamic storage capacity close to the upper bound of the static storage capacity. The difference in these two estimates for dynamic storage capacity stems from time-dependent pressure attenuation which is more effective in the latter calculation. As mentioned before, this attenuation is due to (1) the pressure-buildup propagation away from the core injection area to the entire model domain, (2) the brine leakage into and through the thick caprock, and (3) the brine flow through the model boundaries, which are open in reality. Without such pressure attenuation, a closed system with high permeability has a constant dynamic storage capacity, whether increasing injection rate or time.

Obviously, considering the necessary time frame (50 to 100 years) for global climate change mitigation, a storage scenario involving an injection period of 1200 years is not an option. In the other scenario, where a higher injection rate is assumed, the pressure buildup in the core injection area is a limiting factor for dynamic storage capacity, even when the pressure bleed-off effects are considered. In the base case, the contributions to accommodating the 5.43 km^3 resident brine displaced by free-phase and dissolved CO_2 at 50 years include (1) a 2.49 km^3 pore volume made available by pressure buildup and related pore and brine compressibilities in the core injection area, (2) a 1.19 km^3 pore

8

volume in the model domain outside of the core injection area, again caused by pressure buildup and related compressibilities, (3) a 1.22 km^3 pore volume in the caprock, (4) a 0.49 km^3 cumulative brine volume migrated into overlying aquifers through the caprock, and (5) a 0.04 km^3 cumulative fluid volume migrated laterally out of the model domain. While these total volumes of fluid migration are large, they correspond to very small flow velocities and displacement lengths that would not cause environmental concerns [6]. For example, the average flow velocity across the lateral boundary of the model domain is less than 0.01 mm/year, and the maximum rate of fluid migration through the caprock is only 0.65 mm/year. For the upscaled case with a dynamic storage capacity of 18.1 Gt CO_2, the storage efficiency (relative to the most suitable pore volume of 1419.5 km^3 in the core injection area) is 1.38%. In contrast, if the core injection area was acting as a closed hydrogeological system, the (static) storage efficiency would be 0.63% at best.

4.2. The Southern San Joaquin Basin: A Partially Closed System

In the southern San Joaquin Basin, the deep Vedder Sand has been considered as an important target formation for GCS in California (see Figure 3). The formation pinches out towards the south, north, and west. To the east, the Vedder Sand (and its equivalent sandstones) outcrops along the edge of the Sierra Nevada mountain range. Its salinity is relatively modest, ranging from 29,000 mg litre^{-1} in the deeper portions of the formation to less than 100 mg litre^{-1} in the outcrop region. As a result, we use the term "water" in this subsection to refer to the resident fluid of variable salinity. The primary seal is formed by the Temblor-Freeman shale, except in the northern area where the Vedder Sand connects with the overlying Olcese Sand, another possible storage formation. Numerous oilfields exist in the basin, with their oil/gas pools in different formations, including the Vedder Sand. The oilfields act like closed, partially closed, or open subsystems, evidenced by strong variations in pressure behavior observed during petroleum extraction. For example, the pressure decrease (induced by production of petroleum and produced water) observed at wells and the subsidence imaged using InSAR data indicate that the Kern River oilfield is a closed subsystem bounded by faults and a formation outcrop [23-24]. In summary, the Vedder Sand in the southern San Joaquin Basin forms a partially closed storage system with three closed boundaries and one open boundary, and comprises some localized, fault-bounded closed and partially closed subsystems. Several major faults may act as partial groundwater barriers to regional groundwater flow.
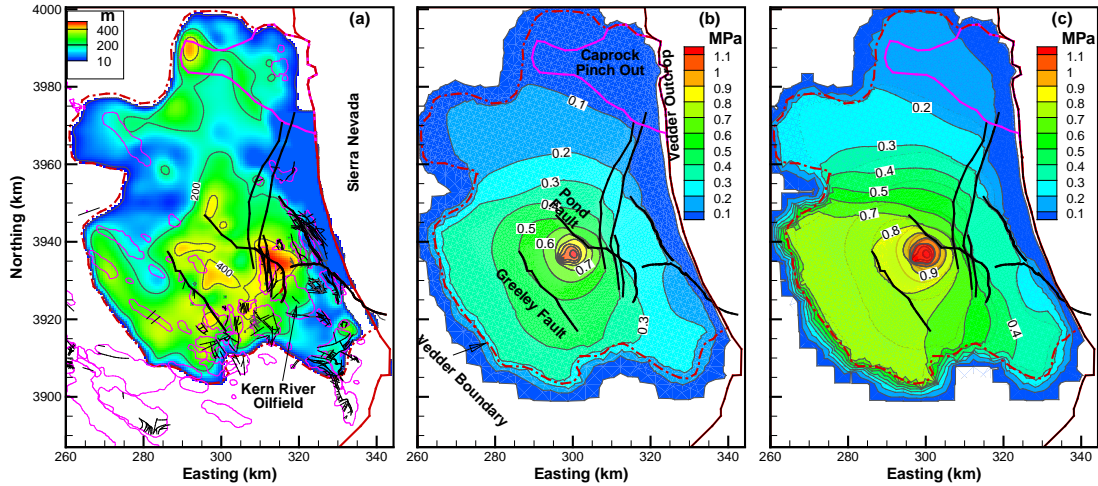
Figure 3. (a) Site map of the southern San Joaquin Basin, including the thickness (m) (in flooded contour) and formation boundary (dashdotted red polygon) of the Vedder Sand, oilfields (pink polygons), area of caprock pinchout (thick pink polygon), minor (black lines) and major (thick black lines) faults, as well as model boundary (thick red polygon). (b) and (c) Simulated pressure buildup (MPa) at 50 years of injection in reference to initial hydrostatic conditions for the base-case seal permeability and a low seal permeability of 10^{-21} m^2, respectively.

A large-scale numerical model of 84 km by 112 km domain size was developed to understand the scale and magnitude of pressure buildup in the partially closed system of the southern San Joaquin Basin. The model represents most of the major geologic and stratigraphic features discussed above. The storage scenario assumes an injection rate of 5 Mt CO_2/year at one well (located between the Greeley and Pond faults) for a period of 50 years. The model accounts for pressure attenuation by diffuse water leakage through seals, by focused water leakage through the seal-pinchout area, and by water discharge into the outcrop area of the storage formation, and also represents the effect of fault zones on pressure-buildup propagation. In addition to the base case (with a caprock permeability of 10^{-18} m^2 and a baserock permeability of 7×10^{-17} m^2), we reduced the cap- and baserock permeability to 10^{-21} m^2 for sensitivity analysis. As shown in Figure 3b (the base case), the pressure perturbation in the Vedder Sand is confined by the southern, western, and northern boundaries of the storage formation at 50 years of injection. The pressure buildup is above 1.10 MPa near the injection center and more than 0.50 MPa in the central area of the basin bounded by the Greeley and Pond faults. In the southwestern region of the storage formation, the pressure buildup is higher than 0.30 MPa, showing the effect of the formation boundaries. The open eastern boundary allows local resident water to flow into shallower formations, without noticeable pressure buildup. Pressure buildup is also less significant in the northern region of the storage formation, because the local absence of the seal there allows water to migrate into overlying aquifers.

The volumetric balance at the end of injection is as follows. The total volume of water displacement includes 333.5×10^6 m^3 displaced by free-phase CO_2 (with an average

density of 656 kg/m^3 of the 218.8 Mt free-phase CO_2) and 25.6×10^6 m^3 by dissolved CO_2. This volume is accommodated by 98.9×10^6 m^3 of pore volume made available by both pore and water compressibilities in response to pressure buildup in the storage formation, 147.6×10^6 m^3 of water migrating from the storage formation into overlying and underlying formations, and 112.6×10^6 m^3 of the water migrating through the Vedder outcrop boundary and through the northern and western open boundaries for all formations except the Vedder Sand. This shows that pressure attenuation by water migration from the storage formation accounts for 72% the additional pore volumes needed to store the injected CO_2 volume.

In comparison to the base case, pressure buildup is higher within the entire storage formation if the seal permeability is too small to allow for pressure relief (see Figure 3c). At the end of injection, the pressure increase compared to initial hydrostatic conditions is above 1.45 MPa near the injection center, over 0.8 MPa in the region between the Greeley and Pond faults, and more than 0.7 in the southwestern region. The total volume of water displaced by free-phase CO_2 (333.0×10^6 m^3) and by dissolved CO_2 (24.9×10^6 m^3) is 357.9×10^6 m^3, very close to that in the base case, indicating that the seal permeability has much less impact on CO_2 plume evolution (as long as there is no CO_2 leakage through the caprock) than on pressure buildup. This total volume of displaced water is accommodated by 160.4×10^6 m^3 pore volume made available by compressibilities in the storage formation, 7.9×10^6 m^3 cumulative water volume leaked through the northern area (where the caprock is absent) and stored in the overlying formations, and 189.6×10^6 m^3 cumulative water volume migrating through the Vedder outcrop boundary and the seal-pinchout area out of the system. The simulation results in both cases indicate that the water outflow from the system is an important mechanism for pressure attenuation, accounting for 31% and 53% of the total displaced water volumes, respectively. Note that the salinity of the outflowing water through the outcrop boundary is very low, and no environmental impact on shallow groundwater resources is expected.

At the end of injection (the base case), the injected CO_2 mass (250 Mt in total) is safely stored in the storage formation, either as dissolved CO_2 (31.2 Mt) or as free-phase CO_2 (218.8 Mt). The CO_2 plume is located between the Greeley and Pond faults. With time, the plume of free-phase CO_2 continues to migrate updip while more and more CO_2 becomes trapped. Simulation results show that at 1000 years, the total injected CO_2 mass is safely contained in the storage formation, either by residual trapping (189.6 Mt) or by dissolution trapping (60.4 Mt), leaving no mobile free-phase CO_2 in the model domain.

5. Discussion

As demonstrated by the two examples above, whether a system is effectively open or closed with respect to assessing dynamic storage capacity depends on the dimensions of the system and the scale of pressure perturbation. For the Illinois Basin, Birkholzer and Zhou[6] simulated pressure buildup in the entire model domain, using boundary conditions

representing an open system and alternatively a closed system. It was found that both cases produce essentially identical solutions over 50 years of injection. After CO_2 injection stops, the pressure perturbation eventually arrives at the boundaries of the model domain (a result of the system slowly approaching a new pressure equilibrium), which was truncated laterally from the more extensive open system. It appears that the assumption of an open system does not have a significant effect on the estimated dynamic storage capacity, which depends mostly on pressure buildup at the end of injection.

The southern San Joaquin Basin is a partially closed system, because the storage formation pinches out in all directions except along the eastern outcrop boundary. Pressure increases with injection time along the closed western and southern boundaries of the Vedder Sand. However, the pressure buildup is attenuated because of the flow of displaced water towards the eastern outcrop area, the diffuse leakage through the overlying and underlying seals, and the upward flow in the area where the caprock is absent. The model domain covers all real hydrogeologic boundaries of the storage formation. The formation boundaries and their associated conditions can be easily implemented in the model, without necessity to make assumptions about a closed or an open system.

In contrast, Ehlig-Economides and Economides[1] envisioned that storage formations are completely closed laterally and vertically, and that simulations assuming an open system violate the requirement of storage security and are therefore generally wrong. They disregarded the possibility of pressure attenuation by brine displacement in laterally extensive aquifers and also neglected the effect of pressure bleed-off caused by diffuse/focused brine migration through sealing units. For their closed system analysis, the maximum storage efficiency was estimated to be 1% (dependent only on pore and brine compressibilities and maximum tolerable pressure buildup), which was calculated using a newly developed analytical solution. The analytical solution works well, and can be used to reproduce the simulation results presented in earlier work for similarly closed systems (Zhou et al. [3]). However, there is a central difference between the two papers. Zhou et al. [3] considered the closed system as an end-member case of geologic systems and pointed out that the semi-closed or open systems are generally more representative of deep saline formations than the closed-system case. They demonstrated that over the large footprints affected by pressure perturbation, brine will be able to flow into and through the overlying and underlying seals in sufficient volumes to considerably reduce pressure effects in a semi-closed storage reservoir. Birkholzer et al.[7] also observed strong pressure bleed-off through seals for an idealized open system with relatively low seal permeabilities. For GCS to be successful at a large scale, the large storage potential of open and semi-closed systems will need to be utilized, where the dynamic storage capacity is enhanced by benefiting from various pressure-attenuation mechanisms.

Generally, model simulations evaluating pressure buildup and thus dynamic storage capacity need to ensure proper definition of lateral and vertical boundary conditions. Any storage formation or sedimentary basin is in fact limited in its lateral dimensions, having either (close-to) impervious or open (e.g., at outcrops) natural boundaries, and may include a number of closed subsystems (e.g., fault-bounded oilfields). When pressure buildup induced by CO_2 injection has not reached these natural boundaries during the injection period, the system can be assumed open, and a truncated model domain can be chosen for storage capacity assessment. When the model domain is large enough to cover the natural boundaries of a storage formation, the corresponding conditions (either fixed-pressure or no-flow) should be used, so that there is no necessity to make assumptions about open or closed systems.

6. Conclusions

This discussion presents (1) the scale of pore volumes needed for future GCS deployment in terms of injection rates and cumulative volumes in comparison to existing injection-extraction activities, (2) a simple estimation of the extent of pressure buildup induced by industrial-scale CO_2 injection and storage, (3) the simulated pressure buildup in response to future GCS scenarios in two example sedimentary basins, and (4) a comparison of pressure response in open and closed subsurface systems. Our modeling studies over the last few years have led us to the following understanding of pressure buildup in geologic carbon sequestration: (1) the pressure buildup in response to CO_2 storage may be a limiting factor in determining dynamic storage capacity of a sedimentary basin, because very large volumes of subsurface pore space are needed for GCS to play an important role in climate change mitigation, (2) the pressure buildup induced by GCS may be attenuated through diffuse leakage through low-permeability seals, propagation of pressure buildup away from injection areas to margins of the sedimentary basin, and brine leakage through localized fast-flow pathways (e.g., seal pinchout areas, leaky faults, and leaky wells), and (3) model predictions of pressure buildup need to include such attenuation effects in order to derive realistic estimates of dynamic storage capacity. The latter implies that the assumption of CO_2 storage reservoirs acting as closed sub-systems, an assumption made for example by Ehlig-Economides and Economides[1], needs to be carefully evaluated against the regional-scale hydrogeologic conditions that allow for pressure attenuation. Pressure management may be undertaken to relieve a GCS-pressurized system through passive wellbore leakage and/or active brine extraction from the storage formation.

The project is jointly coordinated by NETL and the U.S. Environmental Protection Agency.

References

1. Ehlig-Economides C and Economides MJ, Sequestering carbon dioxide in a closed underground volume. *J. Petrol. Sci. Eng.* **70,** 123–130 (2010).

2. IPCC (Intergovernmental Panel on Climate Change), *IPCC Special Report on Carbon Dioxide Capture and Storage*. Cambridge University Press, New York (2005).

3. Zhou Q, Birkholzer JT, Tsang CF and Rutqvist J, A method for quick assessment of CO_2 storage capacity in closed and semi-closed saline formations. *Int. J. Greenh. Gas Con.* **2**(4), 626-639 (2008).

4. Nicot JP, Evaluation of large-scale CO_2 storage on fresh-water sections of aquifers: An example from the Texas Gulf Coast Basin. *Int. J. Greenh. Gas Con.* **2**(4), 582–593 (2008).

5. Birkholzer JT and Zhou Q, Basin-scale hydrological impacts of CO_2 storage: Regulatory and capacity implications. *Int. J. Greenh. Gas Con.* **3**(6), 745-756 (2009).

6. Zhou Q, Birkholzer JT, Mehnert E, Lin YF and Zhang K, Modeling basin- and plume-scale processes of CO_2 storage for full-scale deployment. *Ground Water* **48**(4), 494-514 (2010).

7. Birkholzer JT, Zhou Q and Tsang CF, Large-scale impact of CO_2 storage in deep saline aquifers: A sensitivity study on pressure response in stratified systems. *Int. J. Greenh. Gas Con.* **3**(2), 181-194 (2009).

8. Kaldi J and Bachu S, Geologic carbon sequestration: Prediction and verification, AAPG/SEG/SPE Hedberg Conference, August 16-19, 2009, Vancouver, Canada (2009).

9. USDOE (U.S. Department of Energy), Carbon sequestration atlas of the United States and Canada, 2nd Ed., National Energy Technology Laboratory, Pittsburgh, PA, USA (2008).

10. Khatib Z and Verbeek P, Water to value – produced water management for sustainable field development of mature and green fields. *J. Petrol. Technol.* **55**(1), 26-28 (2003).

11. Veil JA, Puder MG, Elcock D and Redweik Jr. RJ, A white paper describing produced water from production of crude oil, natural gas, and coal bed methane, Argonne National Laboratory, IL, USA (2004).

12. Clark CE and Veil JA, Produced water volumes and management practices in the United States, ANL/EVS/R-09/1, Argonne National Laboratory, IL, USA (2009).

13. Kenny JF, Barber NL, Hutson SS, Linsey KS, Lovelace JK and Maupin MA, Estimated use of water in the United States in 2005: U.S. Geological Survey Circular 1344, pp 52, USA (2009).

14. USEIA (U.S. Energy Information Agency), http://www.eia.gov/.

15. Birkholzer JT, Zhou Q and Wagoner JL, Behavior of pressure buildup in a partially compartmentalized system. *Int. J. Greenh. Gas Con.* (submitted) (2011).

16. Nordbotten JM, Celia MA and Bachu S, Analytical solutions for leakage rates through abandoned wells. *Water Resour. Res.* **40**, W04204 (2004).

17. Zhou Q, Birkholzer JT and Tsang CF, A semi-analytical solution for large-scale injection-induced pressure perturbation and leakage in a laterally bounded aquifer-aquitard system. *Transport Porous Med.* **78**(1), 127-148 (2009).

18. Crank J, *The Mathematics of Diffusion*, 2nd ed., Oxford University Press, Oxford, United Kingdom (1975).

19. Neuzil CE, How permeable are clays and shales? *Water Resour. Res.* **30**(2), 145-150 (1994).

20. Zhou Q, Birkholzer JT, Wagoner JL, Wang Y and Zhang K, The role of fault zones in geologic carbon sequestration: An application to the southern San Joaquin Basin, California (submitted) (2011).

21. Pruess, K, ECO2N: A TOUGH2 fluid property module for mixtures of water, NaCl, and CO2. LBNL-57952, Lawrence Berkeley National Laboratory, Berkeley, CA, USA (2005).

22. Pruess K, Oldenburg CM, and Moridis G, TOUGH2 user's guide. Report LBNL-43134, Lawrence Berkeley National Laboratory, Berkeley, CA, USA (1999).

23. Coburn, MG and Gillespie JM, A hydrogeologic study to optimize steamflood performance in a giant oilfield: Kern River field, California, AAPG Bulletin, **86**(8), 1489 – 1505 (2002).

24. Snieder R, Hubbard S, Haney M, Bawden G, Hatchell P et al, Advanced noninvasive geophysical monitoring techniques, *Annu. Rev. Earth Planet. Sci.* **35**, 653–83 (2007).

DISCLAIMER